RSC Advances

PAPER

View Article Online
View Journal | View Issue

Cite this: *RSC Adv.*, 2016, **6**, 25393

Lead adsorption from aqueous solutions by a granular adsorbent prepared from phoenix tree leaves

Sha Liang, Nan Ye, Yuchen Hu, Yafei Shi, Wei Zhang, Wenbo Yu, Xu Wu and Jiakuan Yang*

In this study, a granular adsorbent was prepared from phoenix tree leaf powder with bentonite as the binder. The granular adsorbent was characterized by TG, BET and SEM analyses. The maximum specific surface area and pore volume were 166.3 $m^2\ g^{-1}$ and 0.276 $cm^3\ g^{-1}$, respectively, after the granular adsorbent was calcined at 500 °C. Effects of pH, adsorption time and initial metal ion concentration on the adsorption of Pb^{2+} by 500 °C calcined granular adsorbent were investigated in batch experiments. Higher pH was favorable for the adsorption process and significant release of Na^+, K^+ and Mg^{2+} were observed, assuming the predominant Pb^{2+} adsorption mechanism was ion exchange. The adsorption could attain equilibrium within 24 h with a gradual increase of the solution pH. The kinetics data were analyzed using three adsorption kinetic models: the pseudo-first-order, pseudo-second-order and intraparticle diffusion equations. Results show that intraparticle diffusion or chemical adsorption is the rate-limiting step depending on the adsorption time. The adsorption isotherms best fitted the Langmuir–Freundlich model and the maximum Langmuir adsorption capacity was found to be 71 mg g^{-1}. This novel granular adsorbent has proven to be a potential inexpensive adsorbent for Pb^{2+} removal from aqueous solutions.

Received 4th February 2016
Accepted 1st March 2016

DOI: 10.1039/c6ra03258c

www.rsc.org/advances

1. Introduction

Pollution of water resources by toxic heavy metals, such as mercury, lead, copper, chromium, nickel, cadmium and zinc, has raised great concern in recent decades. These heavy metals are potentially hazardous to humans and aquatic species. Stringent limits have been imposed on potable water supplies as well as effluent discharge. Elevated heavy metal concentrations can be reduced by chemical precipitation, membrane filtration or ion exchange. However, for concentrations below 100 mg L^{-1}, these methods are less effective, more costly and/or difficult to meet the limits. Using inexpensive biomass as adsorbents to remove heavy metals from wastewater has been considered as an economical and environment friendly alternative recently.[1,2]

Phoenix tree (or *Firmiana simplex*) is commonly used for landscaping in major streets, parks and campus of schools in China. A lot of phoenix tree leaves fall in deep autumn that imposes a great burden on street sweeping. These fallen leaves are mainly landfilled or incinerated. They take up spaces in landfill; and incineration of leaves may release fume, dusts and other potentially harmful gases. Beneficial reuses of them will minimize their adverse environmental impact from disposal. Similar to other agricultural wastes, fallen phoenix tree leaves are mainly composed of cellulose, hemi-cellulose, lignin and a variety of extractives. All of them contain various functional groups, such as carboxyl and hydroxyl, which make adsorption processes possible. Phoenix tree leaves have been proven to effectively remove methylene blue,[3,4] Pb(II),[5] Mn(II),[6] Cd(II)[7] and Zn(II)[8] from aqueous solutions.

Adsorbents can be in the form of powder, gel or suspension, which can provide a large surface area and a high capacity for adsorption. However, serious operational problems such as pore clogging, excessive pressure drop and mass loss make then unsuitable for direct use in packed beds. In addition, large sedimentation basins or filtration may be needed to recover/remove these adsorbents.[9,10] Thus, powdered adsorbents need to be stabilized, fixed or granulated before they can be used in most practical adsorption applications. Granulation is a process to mix the adsorbent powder with a binder, using manual, vibration-dropping, spray coating or extrusion methods. Commercial granular activated carbon has been reported to remove heavy metal ions and dye from aqueous solutions,[11,12] but the cost to prepare the granular activated carbon is high. To use the waste biomass powder to prepare granular adsorbent is seldom reported.

Bentonite is a natural clay with a general chemical formula of $Na_x(Al,Mg)_2SiO_{10}(OH)_2 \cdot nH_2O$. China is ranked first in the

School of Environmental Science and Engineering, Huazhong University of Science and Technology (HUST), Wuhan, Hubei, 430074, PR China. E-mail: jkyang@mail.hust.edu.cn; Fax: +86 27 87792102; Tel: +86 27 87792207

world with regards to bentonite reserves. It is also the traditional low-cost efficient adsorbent, which has high potential for heavy metal removal from wastewater due to its abundance, chemical and mechanical stability, large specific surface area, high cation exchange capacity, and unique structural properties.[13] In some studies, bentonite was used as a porous based support material to enhance the dispersibility of nanoscale zero-valent iron for the removal of hexavalent chromium from wastewater.[14]

In this study, fallen phoenix tree leaves were used as the raw material for preparation of a novel granular adsorbent with bentonite as the binder. The batch adsorption behaviors of the prepared granular adsorbent for removing Pb^{2+} from aqueous solutions were investigated.

2. Materials and methods

2.1 Materials

All chemicals used were of analytical grade. The Pb stock solution was prepared from $Pb(NO_3)_2$ with deionized water. Solutions containing Pb ions were freshly prepared by diluting the Pb stock solution with deionized water.

Fallen phoenix tree leaves were collected from the university campus in last autumn. After air dried, the fallen leaves were crushed by a cutting mill and then the powder was passed a sieve of 60 mesh (effective opening size of 0.25 mm). The results of an elemental analysis of leaf powder were N 0.65%, C 44.46%, H 5.95%, S 0.36% and O 41.56% by wt (oxygen was determined from the difference).

Bentonite was obtained from a local chemical company. The raw bentonite was sieved through a 200 mesh screen prior to use. The results of chemical compositions of the bentonite samples are depicted in Table 1. As shown, the main chemical components of the bentonite are SiO_2, Al_2O_3, Na_2O, Fe_2O_3, MgO, K_2O and CaO.

2.2 Preparation of granular adsorbent

Equal amounts of phoenix tree leaf powder and bentonite were weighed and mixed first. Deionized water was then slowly added into the mixture until a homogeneous paste was formed. The paste was then manually made into granules with a diameter of 5–6 mm and air dried. The granules were then calcined in a tube furnace under N_2 atmosphere at 200 °C, 300 °C, 400 °C, 500 °C and 600 °C for 1 h, respectively. The color of the calcined granular adsorbents turned from brownish yellow to dark black with an increasing calcination temperature. In the test experiments, the air dried raw granular adsorbent will slowly disintegrate in water after several hours while the calcined granular adsorbents can maintain their shape after being soaked in water for 24 h.

2.3 Adsorption experiments

Batch adsorption experiments were carried out by shaking 200 mg of the granular adsorbent with 40 mL of Pb^{2+} solutions of certain concentration in a water bath shaker (150 rpm and 30 °C) for a specific time. After adsorption and filtration, the concentrations of metal ions in the filtrate solution were analyzed by using inductive coupled plasma emission spectrometer (Optima 8300 ICP-OES, PerkinElmer). The amount of metal adsorbed (q_e, mg g^{-1}) was determined by using the following equation:

$$q_e = \frac{(C_0 - C_e)V}{m} \quad (1)$$

where, C_0 and C_e represent the initial and equilibrium Pb^{2+} concentrations (mg L^{-1}), respectively; V is the volume of the solution (L) and m is the amount (g) of adsorbent. In the test experiments, under the same adsorption conditions (initial Pb^{2+} concentration: 100 mg L^{-1}, adsorption time: 24 h, solid/liquid ratio: 5, pH: 5.0–5.5, 150 rpm, 25 °C), the adsorption efficiencies for Pb^{2+} by bentonite, leaf powder and calcined composite product (calcined at 300 °C) were 86.9%, 84.3% and 99.2%, respectively. So, the calcined granular adsorbent showed the best removal efficiency. And the main problem to use bentonite and leaf powder was that they were in the form of powder which was difficult for filtration and separation.

2.4 Characterizations of adsorbents

The thermal analysis of the raw phoenix tree leaf powder, bentonite and the granular adsorbent were performed in a Pt crucible by thermo gravimetric analysis (TG) using a simultaneous thermal analyzer (TA-Q600, USA) in the range of 10–800 °C and at a ramping rate of 10 °C min^{-1} under a nitrogen atmosphere with gas flow rate of 100 mL min^{-1}.

Specific areas of the prepared granular adsorbents calcined at different temperatures were measured by a static nitrogen adsorption analyzer (JW-BK122W, Beijing JWGB Sci&Tech. Co., Ltd, China).

Table 1 Chemical compositions of the bentonite specimen (wt%)

SiO_2	Al_2O_3	Na_2O	Fe_2O_3	MgO	K_2O	CaO	TiO_2	P_2O_5	SO_3
67.022	15.038	3.285	2.152	1.898	1.447	1.369	0.329	0.080	0.057
MnO	Rb_2O	SrO	Y_2O_3	ZrO_2	BaO	PbO	Cl	As_2O_3	LOI[a]
0.044	0.010	0.023	0.002	0.022	0.021	0.008	0.041	0.007	7.146

[a] LOI: loss of ignition at 1200 °C.

Morphologies of the raw granular adsorbent, the granular adsorbent calcined at 500 °C and the Pb^{2+}-loaded granular adsorbent were studied with scanning electron microscopy (Sirion 200SEM, FEI, Holland) operated at 10 kV after the samples were coated with gold.

3. Results and discussion

3.1 Characterizations of granular adsorbent

3.1.1 Thermogravimetric analysis. The thermal analysis of the phoenix tree leaf powder, bentonite and the raw granular adsorbent are shown in Fig. 1. From Fig. 1(a), the thermogravimetric profile obtained for phoenix tree leaf powder (Fig. 1(a)) can be divided into three stages of mass loss. The first stage starts from the beginning until about 140 °C, which corresponds to water loss. The second stage, ranging from 140 °C to 550 °C, corresponds to decomposition of organic matters as well as release of volatile substances from decomposition of inorganic compounds. During this stage, the complete degradation of cellulose occurs (about 300 °C). Lignin pyrolysis occurs at about 400 °C, while hemicellulose decomposes at a considerably lower temperature.[15] The temperature ranges for pyrolysis of three types of components overlap each other. Thus continuous rate peaks can be observed in the DTG curves. The fastest weight loss rate of 0.34% per °C occurs at 342 °C. Finally, the third stage, ranging from 550 °C to 800 °C represents the further decomposition of lignin and generation of carbon and ash residues.

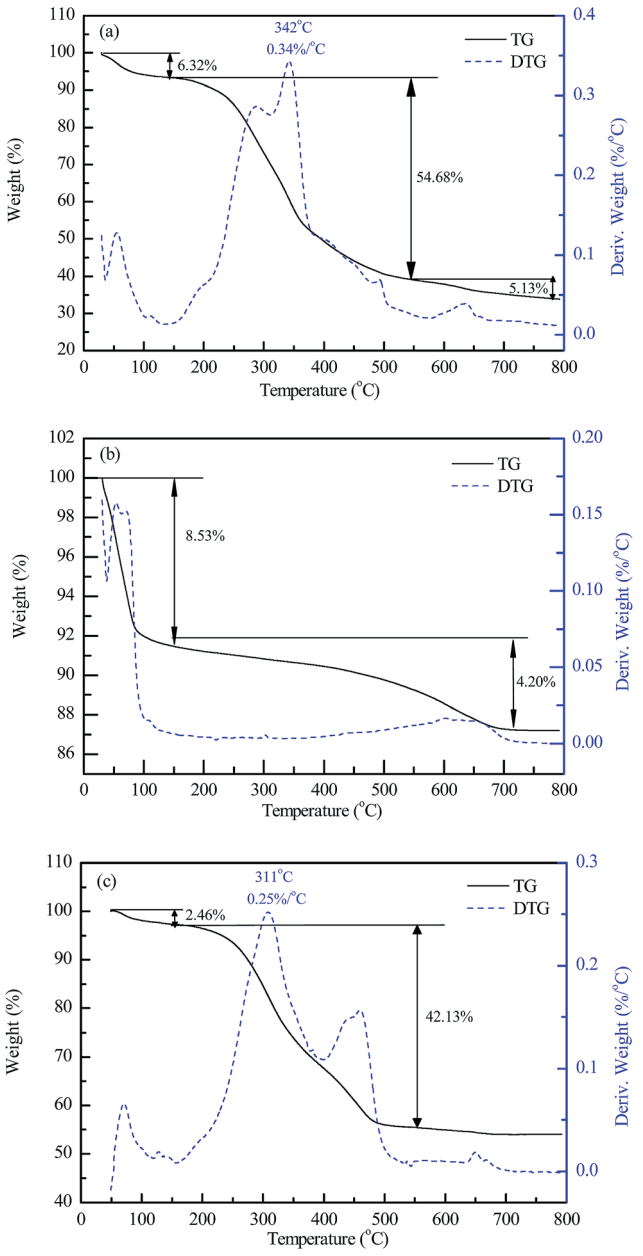

Fig. 1 TG–DTG curves of (a) raw phoenix tree leaf powder, (b) bentonite and (c) raw granular adsorbent.

As shown in Fig. 1(b), the weight loss of bentonite under 800 °C is only about 12%. The TG curve presents two stages of mass loss. The first stage corresponds to the evaporation of surface and interlayer absorbed water (8.53%). The second stage corresponds to the removal of structural water (4.2%).

From Fig. 1(c), the TG–DTG curves of the raw granular adsorbent are similar to that of phoenix tree leaf powder, except that the weight loss in each stage of the TG curve is smaller than the corresponding one in the raw phoenix tree leaf power. In addition, the position and intensity of weight loss rate peaks in the DTG curve held towards earlier and lower (0.25% per °C at 311 °C) by the presence of bentonite.

The weight loss percentages of granular adsorbents calcined at 200 °C, 300 °C, 400 °C, 500 °C and 600 °C under N_2 atmosphere for 1 h were 11.5%, 25.5%, 29%, 36% and 35%, respectively. This result is consistent with Fig. 1(c) in which the TG curve becomes flatter after 500 °C. But the weight loss percentage of the granular adsorbent is less than the theoretical value from TG curve, which implies that the pyrolysis was not completed.

3.1.2 Specific surface area. Specific surface areas of the prepared granular adsorbents calcined at different temperatures were measured by a static nitrogen adsorption analyzer. The results are given in Table 2. The specific surface area of the raw granular adsorbent dried at 65 °C is 8.1 $m^2\ g^{-1}$. As shown in Table 2, as the calcination temperature increased from 200 °C to 500 °C, the specific surface area of the granular adsorbents increased slightly at first, then rapidly reached the maximum specific surface area of 166.3 $m^2\ g^{-1}$ at 500 °C. It implies that with temperature increased, the decomposition of organic matters and release of volatile substances from decomposition of inorganic compounds resulted in the formation of a lot of pores inside the granular adsorbent. At 500 °C, the organic matters of cellulose, hemicellulose and lignin almost decomposed completely, and the granular adsorbent has the largest total adsorption pore volume as 0.276 $cm^3\ g^{-1}$. When the calcination temperature further increased to 600 °C, the specific surface area became lower, which might be due to the collapse of some micropores from the further decomposition of organic matters.

The nitrogen adsorption/desorption isotherms and pore size distributions of the granular adsorbents calcined at different

Table 2 The results of N_2 adsorption analysis for granular adsorbents calcined at different temperatures

Calcination temperature (°C)	Specific surface area (m^2 g^{-1})	Total adsorption pore volume (cm^3 g^{-1})	Average adsorption pore size (nm)	Micropore volume (cm^3 g^{-1})	Mesopore volume (cm^3 g^{-1})	Most probable pore size (nm)
200	8.5	0.029	14.73	0.0036	0.026	1.262
300	10.3	0.049	17.53	0.0043	0.041	1.264
400	14.7	0.024	7.21	0.0066	0.019	1.244
500	166.3	0.276	5.36	0.0465	0.177	1.077
600	90.1	0.060	3.98	0.0433	0.047	0.981

temperatures are shown in Fig. 2 and 3, respectively. The N_2 adsorption/desorption isotherms (Fig. 2) display similar shapes for the granular adsorbents calcined from 200 to 600 °C, exhibiting the presence of an adsorption hysteresis loop, characteristic of type IV isotherms. Such isotherms are typical of mesoporous solids. On the other hand, the pore size distributions in Fig. 3 denote that the degree of micro-, meso- and macroporosity developments of granular adsorbent calcined at 500 °C are significantly greater than those of the other granular adsorbents.

3.2 Effect of the calcination temperature

Effect of the calcination temperature on the adsorption removal of Pb^{2+} from the aqueous solutions is given in Fig. 4. As shown, the adsorption efficiency and adsorption capacity increase with the increase of temperature from 200 to 500 °C, then decrease afterwards. The highest adsorption efficiency of 99.39% was obtained at 500 °C, which corresponds to the maximum specific surface area and highest adsorption pore volume.

Meanwhile, after adsorption and filtration, the total organic carbon concentrations (TOC) of the filtrate solutions were measured by a TOC analyzer (Multi N/C 2100, Analytic Jena AG, Germany). The TOC concentrations of filtrate solutions after adsorption by granular adsorbents calcined at 200 °C, 300 °C, 400 °C, 500 °C and 600 °C were 241.2, 171.7, 52.8, 24.0 and 4.7 mg L^{-1}, respectively. It can be concluded that the TOC concentrations decrease dramatically with the increase of the calcination temperature. The higher TOC concentrations associated with the low-temperature calcined adsorbents was from the dissolution of pigments and other small molecular weight compounds of the granular adsorbent. This can also be judged from the color of the filtrate, which turns from brownish yellow (200 and 300 °C) to light yellow (400 °C) and to colorless (500 and 600 °C). Therefore, the granular adsorbent calcined at 500 °C were chosen for subsequent experiments.

3.3 Effect of pH

Fig. 5 illustrates the effect of pH on adsorption of Pb^{2+} by the 500 °C-calcined granular adsorbent. It reveals that the adsorption of lead increases from 15 to 99% with an increase in the solution pH from 1.0 to 5.5. The low adsorption efficiency of Pb^{2+} at a lower pH is due to strong H^+ ion competition for the available ion exchange sites. Also, at a low pH, the surface of the granular adsorbent will be more positively or less negatively charged, because of the amphoteric dissociation of oxides of aluminum, silicon, calcium, iron and magnesium presented in bentonite,[16] which does not favor the adsorption of positive-charged lead ions.

Concentrations of other ions including Al^{3+}, Si^{4+}, K^+, Na^+, Ca^{2+}, Mg^{2+} and Fe^{2+} in the filtrate were also measured. As shown in Fig. 5, small amounts of Si^{4+} and Na^+ ions were released into the solution under a stronger acidic environment. At a higher pH, significant releases of light metals including Na^+, K^+ and Mg^{2+} were observed. Also, the final equilibrium pH was higher than the initial pH and reached 6.2 while the initial pH was 5.0.

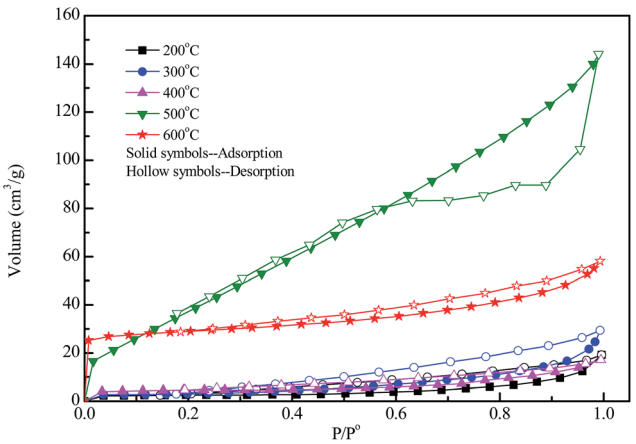

Fig. 2 Nitrogen adsorption–desorption isotherms of the granular adsorbents calcined at different temperatures.

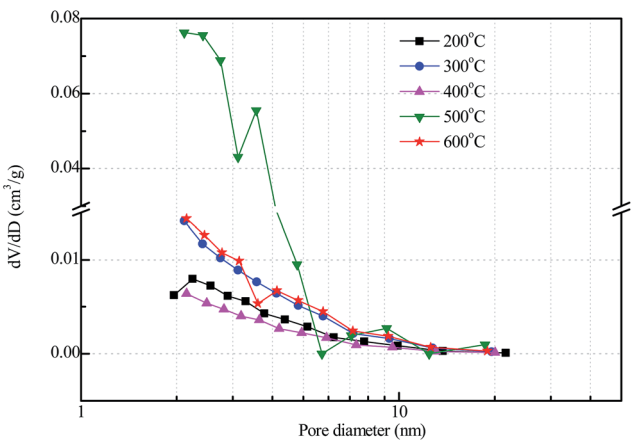

Fig. 3 Pore size distributions of the granular adsorbents calcined at different temperatures.

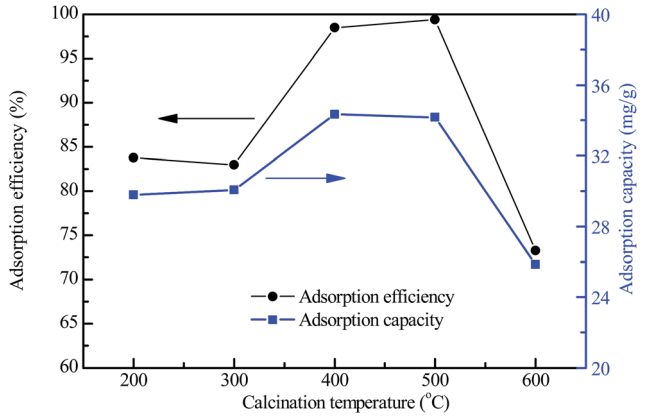

Fig. 4 Effect of calcination temperature on the adsorption of Pb^{2+} by the granular adsorbents. (Initial concentration of Pb^{2+}: 200 mg L^{-1}; solid/liquid: 200 mg/40 mL; initial pH: 5.0–5.5; 30 °C; 24 h).

Thus, ion exchange is considered to be the predominant Pb^{2+} adsorption mechanism. The amounts of metals bound (Pb^{2+} + $1/2H^+$) to the surface of the granular adsorbent and those released ($1/2Na^+ + 1/2K^+ + Mg^{2+}$) under initial pHs of 4, 5 and 5.5 were calculated. The results indicate that the amounts of metals bound (Pb^{2+} + $1/2H^+$) was more than that of released ($1/2Na^+$ + $1/2K^+$ + Mg^{2+}). This implies that other mechanisms such as precipitation and physical adsorption, in addition to ion exchange, could possibly take place.[17]

3.4 Effect of adsorption time

Effect of adsorption time on adsorption of Pb^{2+} by the 500 °C-calcined granular adsorbent and the variations of the solution pH are presented in Fig. 6. As shown, the adsorption efficiency increases with the increase of time until equilibrium reaches at around 20 h. The solution pH increased quickly from 5.0 to around 6.2 in the first two hours, then kept stable afterwards. The reason was that according to the ion exchange mechanism, a certain amount of H^+ was replaced by light metal ions like Na^+, K^+ and Mg^{2+}, which leaded to the increasement of solution pH.

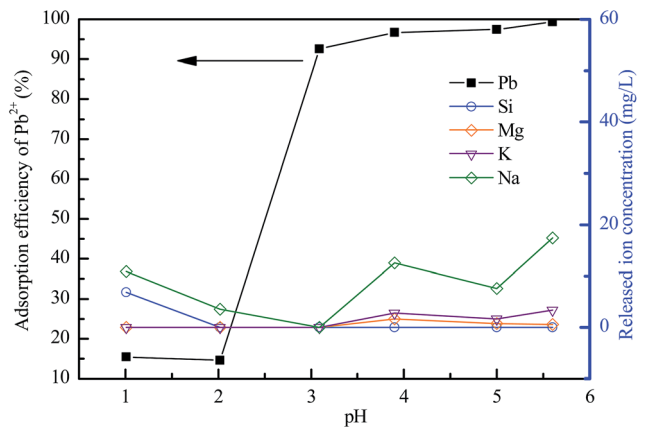

Fig. 5 Effect of pH on the adsorption of Pb^{2+} by the 500 °C-calcined granular adsorbent. (Initial concentration of Pb^{2+}: 200 mg L^{-1}; solid/liquid: 200 mg/40 mL; 30 °C; 24 h).

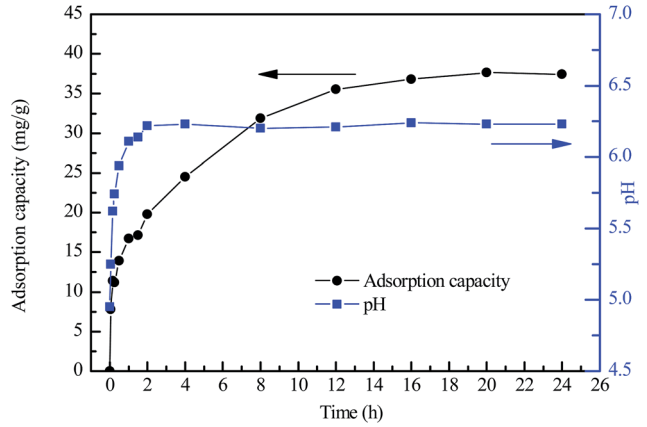

Fig. 6 Effect of adsorption time on the adsorption of Pb^{2+} by the 500 °C-calcined granular adsorbent. (Initial concentration of Pb^{2+}: 200 mg L^{-1}; solid/liquid: 200 mg/40 mL; initial pH: 5.0; 150 rpm; 30 °C).

Generally, the adsorption process can be divided into four stages: (1) bulk transport; (2) film mass transfer; (3) intraparticle diffusion and (4) adsorption. In a rapid stirred, well mixed batch adsorption, mass transport from the bulk solution to the external surface of the adsorbent is usually fast. In addition, film diffusion plays a significant role at shorter time intervals (within first few minutes) and this cannot be considered as the rate limiting step.[18,19] Thus, steps (3) and (4) are the possible rate-limiting steps.

Various models such as pseudo-first- and second-order kinetic equations and intraparticle diffusion equation are used to examine the controlling mechanism of adsorption process.[20,21]

The pseudo-first-order kinetic model known as the Lagergren equation:

$$q_t = q_e\{1 - \exp(-k_1 t)\} \quad (2)$$

where q_t and q_e are the amounts of ion adsorbed at time t and at equilibrium (mg g^{-1}), respectively, and k_1 is the rate constant of pseudo-first-order adsorption process.

The pseudo-second-order kinetic model:

$$q_t = \frac{k_2 q_e^2 t}{(1 + k_2 q_e t)} \quad (3)$$

where k_2 is the equilibrium rate constant of pseudo-second-order adsorption.

The intraparticle diffusion model:

$$q_t = k_{int} t^{1/2} + I \quad (4)$$

where k_{int} is the intraparticle diffusion rate constant and I is the intercept of a plot of q_t *vs.* $t^{1/2}$.

The fitting results of the three kinetics models are plotted in Fig. 7(a). The correlation coefficients (R^2) of pseudo-first-order, pseudo-second-order and intraparticle diffusion model were 0.862, 0.913 and 0.933, respectively. It appears that intraparticle diffusion model provides the best fitting to the experimental data. However, it can be seen from Fig. 7(a) that at adsorption time less

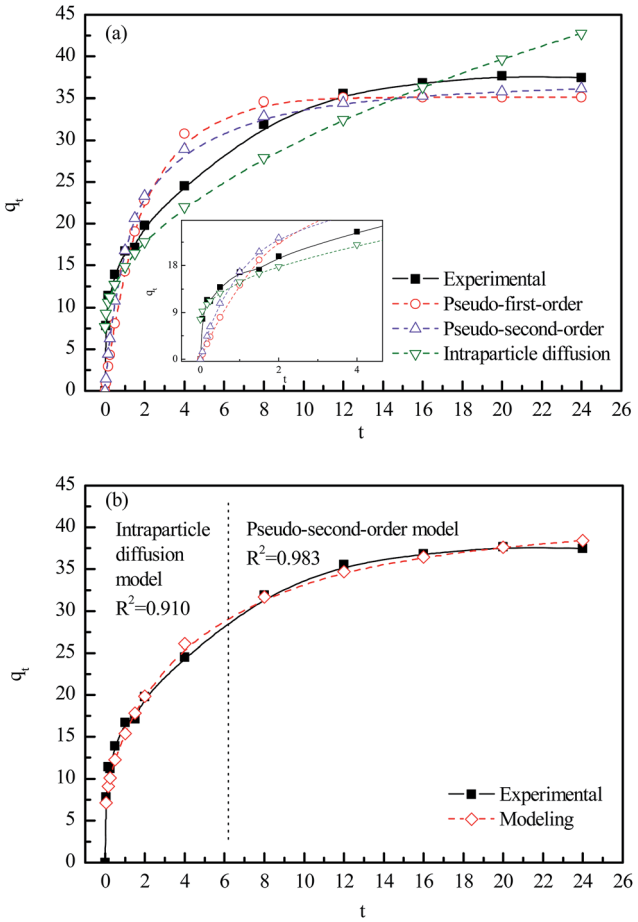

Fig. 7 Adsorption kinetics modeling of Pb^{2+} removal by the 500 °C-calcined granular adsorbent.

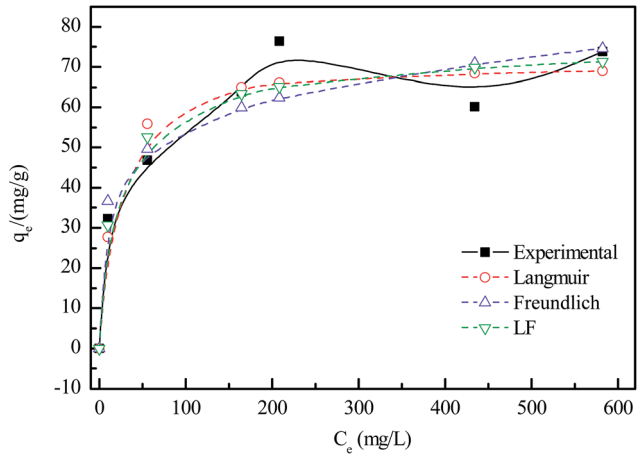

Fig. 8 Adsorption isotherms of Pb^{2+} removal by the 500 °C-calcined granular adsorbent. (Solid/liquid: 200 mg/40 mL; initial pH: 5.0; 30 °C; 24 h).

than 4 h, the intraparticle diffusion model fitted the experimental data very well; at adsorption time more than 4 h, pseudo-second-order model fitted the experimental better than intraparticle diffusion model. This suggests the adsorption process may undergo two stages, at first stage of adsorption time less than 4 h, intraparticle diffusion is the rate limiting step; after then, chemical adsorption is the rate limiting step. Fig. 7(b) plots a satisfactory fitting result of the experimental data by two models.

3.5 Adsorption isotherms

Fig. 8 plots the equilibrium adsorption isotherms between the amount of adsorbed lead ions (q_e) and the equilibrium lead concentration (C_e) in the solution.

The isotherms data were fitted by three isotherm models in the present study: Langmuir, Freundlich and Langmuir–Freundlich (LF) and the fitting results were also shown in the form of dotted lines in Fig. 8.[20,21]

Based on the assumption that all adsorption sites are equivalent and adsorption in active sites is independent of whether the adjacent is occupied, the Langmuir adsorption model can be expressed as:

$$q_e = q_L \frac{K_L C_e}{(1 + K_L C_e)} \quad (5)$$

where q_L is the maximum adsorption capacity of adsorbent, K_L is the Langmuir adsorption constant.

The Freundlich model describes non ideal adsorption or adsorption over heterogeneous surfaces and it is not restricted to monolayer formation, which can be expressed as:

$$q_e = K_F C_e^{1/n_F} \quad (6)$$

where K_F and n are the Freundlich adsorption constants.

The combined features of the both Langmuir and Freundlich models is given by LF model, which can be expressed as:

$$q_e = q_m \frac{K_{LF} C_e^{1/n_{LF}}}{(1 + K_{LF} C_e^{1/n_{LF}})} \quad (7)$$

In eqn (7), if $1/n_{LF}$ becomes 1, then eqn (7) reduces to Langmuir isotherm; at low concentrations, eqn (7) reduces to Freundlich isotherm.

The correlation coefficients (R^2) of Langmuir, Freundlich and LF models were 0.786, 0.749 and 0.814, respectively. So the Langmuir–Freundlich (LF) adsorption isotherm model best fits the experimental data. This means that adsorption of Pb^{2+} on granular adsorbent is occurring by a combined Langmuir–Freundlich model. In other words, adsorption is diffusion

Table 3 Lead adsorption capacity of some biomass based adsorbents reported in the literatures

Adsorbent	q_m (mg g^{-1})	References
Granular adsorbent prepared from phoenix tree leaf	71	This study
Firmiana simplex leaf (phoenix tree leaf)	137	5
Grape bagasse	42	15
Sago processing waste	47	22
Mango peel waste	99	23
Orange peel	90	24
Tea waste	65	25
Maize bran	143	26

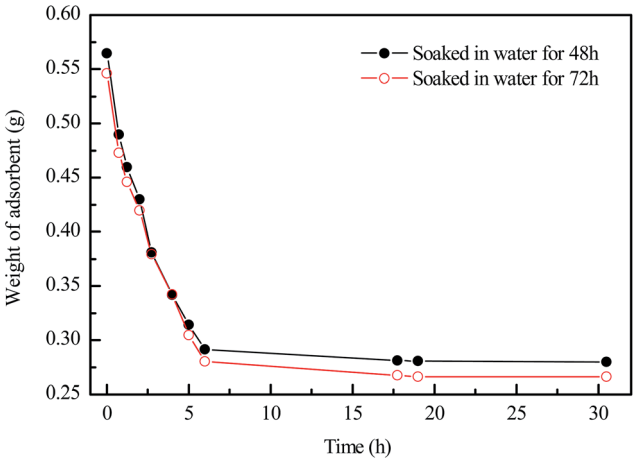

Fig. 9 Variations of the weight of soaked adsorbents after 48 and 72 h of immersion.

controlled at low lead concentrations while monomolecular adsorption with a saturation value takes place at high lead concentrations.

The maximum adsorption capacity of Pb^{2+} on the granular adsorbent is 71 mg g^{-1}, calculated by Langmuir model. A comparison of adsorption capacity of Pb^{2+} by some biomass based adsorbents was given in Table 3.

3.6 Swelling behavior of granular adsorbent

According to literature,[27] biochar will swell in water to expand internal volume. To study the swelling behavior, around 0.28 g of the dry calcined granular adsorbent was immersed into distilled water for 48 and 72 h, respectively. Then the soaked granular adsorbent was placed on a preweighed filter and all the surface water was removed using suction filtration. The weight of the adsorbent was recorded periodically to obtain the weight loss as a function to time (Fig. 9). The weight losses of the adsorbent due to internal water evaporation after both 48 and 72 h soaking time were the same as 0.28 g, which means internal water occupied about 1 g g^{-1} adsorbent. The internal pore volume could have occurred by water diffusion into pore walls and expansion of internal pore structure.

The SEM images show that after calcination at 500 °C (Fig. 10(b)), surface of the granular adsorbent becomes more porous and rough than the raw granular adsorbent (Fig. 10(a)) due to the removal of volatile material as discussed in Section 3.1.1. After adsorption of Pb^{2+} (Fig. 10(c)), the granular adsorbent exhibits even more porous and irregular morphology due to the further opening of internal pores by swelling in water.

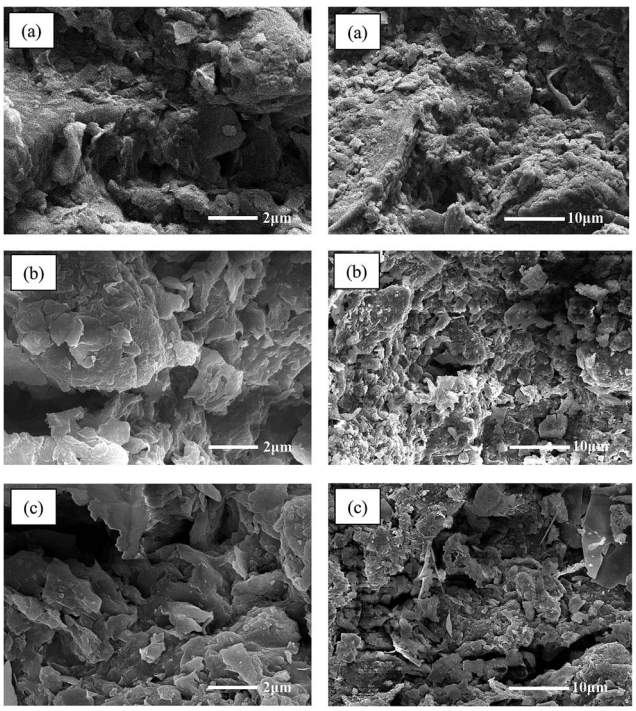

Fig. 10 The SEM images of granular adsorbents: (a) uncalcined, (b) calcined at 500 °C, and (c) after adsorption of Pb^{2+}.

4. Conclusions

In this study, the granular adsorbent prepared from phoenix tree leaf powder with bentonite as the binder has proven to be a potential inexpensive adsorbent for Pb^{2+} removal from aqueous solutions. The granular adsorbent was characterized by TG, BET and SEM analyses. The thermogravimetric profile shows three stages of mass loss. The maximum specific surface area and pore volume were 166.3 m^2 g^{-1} and 0.276 cm^3 g^{-1}, respectively, when the granular adsorbent was calcined at 500 °C. The adsorption behaviors for Pb^{2+} by 500 °C-calcined granular adsorbent were investigated in batch studies to study the effects of pH, adsorption and initial metal ion concentration. The results show that the maximum batch adsorption capacity of Pb^{2+} by the 500 °C-calcined granular adsorbent was 71 mg g^{-1}. For practical application, the column adsorption behaviors of this novel granular adsorbent will be studied in our future work.

Acknowledgements

This work was financially supported by the Natural Science Foundation of China for the Youth (51404106), the Youth Innovation Fund from Huazhong University of Science and Technology (2014QN149), project of Innovative and Interdisciplinary Team, Hust (0118261077) and Wuhan Planning Project of Science and Technology, China (2015070404010200). The authors would also like to thank the Analytical and Testing Center of Huazhong University of Science and Technology, for providing the facilities for the experimental measurements.

References

1 D. Sud, G. Mahajan and M. P. Kaur, *Bioresour. Technol.*, 2008, **99**, 6017–6027.
2 B. Volesky, *Water Res.*, 2007, **41**, 4017–4029.
3 R. Han, W. Zou, W. Yu, S. Cheng, Y. Wang and J. Shi, *J. Hazard. Mater.*, 2007, **141**, 156–162.

4 R. Han, Y. Wang, X. Zhao, Y. Wang, F. Xie, J. Cheng and M. Tang, *Desalination*, 2009, **245**, 284–297.
5 Z. Li, X. Tang, Y. Chen, L. Wei and Y. Wang, *J. Hazard. Mater.*, 2009, **169**, 386–394.
6 Z. Li, S. Imaizumi, T. Katsumi, T. Inui, X. Tang and Q. Tang, *J. Hazard. Mater.*, 2010, **177**, 501–507.
7 Q. Tang, X. Tang, M. Hu, Z. Li, Y. Chen and P. Lou, Removal of Cd(II) from aqueous solution with activated *Firmiana simplex* leaf: behaviors and affecting factors, *J. Hazard. Mater.*, 2010, **179**(1), 95–103.
8 Q. Tang, X. Tang, Z. Li, Y. Wang, M. Hu, X. Zhang and Y. Chen, *J. Environ. Eng.*, 2011, **138**, 190–199.
9 C. Zhu, Z. Luan, Y. Wang and X. Shan, *Sep. Purif. Technol.*, 2007, **57**, 161–169.
10 X. Dou, D. Mohan and C. U. Pittman, *Water Res.*, 2013, **47**, 2938–2948.
11 J. Goel, K. Kadirvelu, C. Rajagopal and V. K. Garg, *J. Hazard. Mater.*, 2005, **125**, 211–220.
12 G. Walker and L. Weatherley, *Water Res.*, 1997, **31**, 2093–2101.
13 K. G. Bhattacharyya and S. S. Gupta, *Adv. Colloid Interface Sci.*, 2008, **140**, 114–131.
14 L.-n. Shi, X. Zhang and Z.-l. Chen, *Water Res.*, 2011, **45**, 886–892.
15 N. Farinella, G. Matos and M. Arruda, *Bioresour. Technol.*, 2007, **98**, 1940–1946.
16 S. A. Khan and M. A. Khan, *Waste Manag.*, 1995, **15**, 271–282.
17 D. Mohan, C. U. Pittman Jr, M. Bricka, F. Smith, B. Yancey, J. Mohammad, P. H. Steele, M. F. Alexandre-Franco, V. Gómez-Serrano and H. Gong, *J. Colloid Interface Sci.*, 2007, **310**, 57–73.
18 Y. S. Ho, J. C. Y. Ng and G. McKay, *Sep. Purif. Technol.*, 2000, **29**, 189–232.
19 R. Aravindhan, J. R. Rao and B. U. Nair, *J. Hazard. Mater.*, 2007, **142**, 68–76.
20 S. A. Singh, B. Vemparala and G. Madras, *J. Environ. Chem. Eng.*, 2015, **3**, 2684–2696.
21 S. Liang, X. Y. Guo, N. C. Feng and Q. H. Tian, *J. Hazard. Mater.*, 2010, **174**, 756–762.
22 S. Y. Quek, D. A. J. Wase and C. F. Forster, *Water SA*, 1998, **24**, 251–256.
23 M. Iqbal, A. Saeed and S. Iqbal Zafar, *J. Hazard. Mater.*, 2009, **164**, 161–171.
24 S. Liang, X. Y. Guo, N. C. Feng and Q. H. Tian, *J. Hazard. Mater.*, 2009, **170**, 425–429.
25 B. M. W. P. K. Amarasinghe and R. A. Williams, *Chem. Eng. J.*, 2007, **132**, 299–309.
26 K. K. Singh, M. Talat and S. H. Hasan, *Bioresour. Technol.*, 2006, **97**, 2124–2130.
27 D. Mohan, S. Rajput, V. K. Singh, P. H. Steele and C. U. Pittman Jr, *J. Hazard. Mater.*, 2011, **188**, 319–333.